Video-based analysis of the rotational behaviour of rod-shaped, self-propelled bacteria in holographic optical tweezers

Lena Dewenter, Christina Alpmann, Mike Woerdemann, and Cornelia Denz

Institute of Applied Physics, University of Muenster, Corrensstraße 2/4 Muenster, D-48149 Muenster, Germany

ABSTRACT

Utilising the versatility of holographic optical tweezers and high speed video analysis, we present a scheme for the analysis of the rotational properties of multiple rod-shaped bacteria directly from video microscopy data. The bacterial body and flagella rotation frequency of *Bacillus subtilis* are determined by temporally resolved monitoring of the position of the bacterial body. In contrast to established methods, the video-based approach can be extended to the simultaneous analysis of several bacteria within the field of view. Monitoring multiple bacteria simultaneously will allow resolving the role of hydrodynamic interactions of multiple flagella motors on their mutual dynamics.

Key words: holographic optical tweezers, position detection, biophysical properties, Bacillus subtilis, hydrodynamic interactions, high speed video analysis, bacterial dynamics

1 INTRODUCTION

Many motile species of swimming bacteria feature flagella, i.e. actively driven thin helical filaments, for their movement [1]. Important types of flagella-propelled bacteria include *Escherichia coli* and *Bacillus subtilis*, which are frequently used as prokaryotic (bacterial) model organisms due to their widely studied and well-known biological properties. Both types of bacteria are characterized by a rod-shaped body of a few micrometres and a number of flagella which are individually connected to the body at random positions by a tiny motor [2]. The motor, with its diameter in the order of a few ten nanometres, is one of the smallest known rotational motors, driven by protons or in some cases by ions crossing the transmembrane electrochemical gradient [1,3,4]. The motility of this kind of bacteria is governed by a process called chemotaxis, allowing the bacterium to sense its environment and move accordingly [5]. Chemotaxis takes place in a series of "run" and "tumble" events [5, 6]. When they "run", the cells move steadily forward due to a directed action of the flagella that form a bundle, rotating with a common velocity [6]. When the bundling of the flagella is disturbed, e.g. by one or more flagella changing their direction of rotation, the cell "tumbles" and thus has a high probability to reorient itself towards a new direction in space [6]. The probability of "running" is increased as long as the bacterium senses an increase in advantageous attractants, such as nutritions, and a decrease in repellents, while the probability of "tumbling", and thus reorientation is increased if favoured conditions decline. Following this simple algorithm, the bacterium can approach advantageous living conditions performing a biased "random walk" [5 - 8].

The biophysical properties of the bacterial flagella motor has been intensively studied [3]. In particular, the rotation frequencies of individual flagella and the flagella bundle, respectively, have been investigated intensively as they provide important insight into the motor characteristics. Rotation frequencies of flagella bundles have been measured, for example, by analysis of body vibrations of swimming bacteria [9], by direct observation of fluorescently labelled flagella of swimming [6] or attached [2] bacteria, or by observing bacteria trapped with optical tweezers [7, 10].

While the latter approach of using (single) optical tweezers has the advantage that it defines the position of the optically trapped bacterium under investigation, it is limited to the measurement of a single bacterium at a time. This is due to the fact that the technique relies on time-resolved position detection of a laser beam which is deflected by the trapped bacte-

Biophotonics: Photonic Solutions for Better Health Care III, edited by Jürgen Popp, Wolfgang Drexler, Valery V. Tuchin, Dennis L. Matthews, Proc. of SPIE Vol. 8427, 84270N

rium. The deflected laser beam carries information on the position and thus the rotation state of the bacterium and the flagella bundle. While it is possible to create multiple optical tweezers simultaneously, for example using the technique of holographic optical tweezers [11], it is not straightforward to detect the position of multiple bacteria at the same time by means of the deflected laser beams.

Comparing of simultaneously measured rotational properties of different bacteria, however, is crucial to obtain relevant insights in hydrodynamic interactions of multiple nano motors [12]. Aiming at the investigation of possible cooperative effects, a new method for the simultaneous rotational analysis of several bacteria is presented. Using high-speed video microscopy methods and appropriate digital post processing, we demonstrate the analysis of the rotation rate of the bacterial body and its flagella by its power spectrum [10]. This method is in principle not limited to a single bacterium at a time but provides the potential to monitor multiple bacteria simultaneously.

For this proof-of-concept study we utilise holographic optical tweezers (HOT) based on computer-generated light patterns in order to trap multiple bacteria at the same time in defined configurations [11]. As a model bacterium, we employ a wild type strain of *B. subtilis*, a rod-shaped bacterium with diameters of about 1µm and length of 2-3 µm.

2 HOLOGRAPHIC OPTICAL TWEEZERS SYSTEM

The optical micromanipulation system [11] consists of in-house developed holographic optical tweezers integrated into a commercial Nikon Eclipse Ti inverted fluorescence microscope, as shown in figure 1.

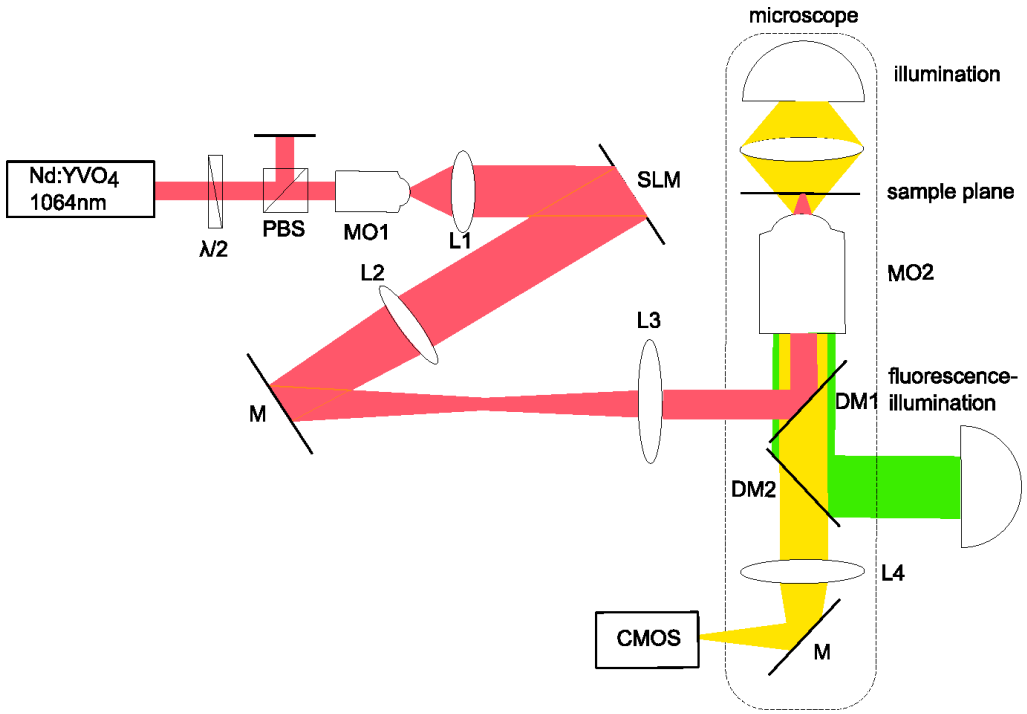

Figure 1. Holographic optical tweezers system (HOT); Nd:YVO_4: solid state cw-laser (Yttrium-Vanadat, Nd doping) λ/2: half-wave plate, PBS: polarising beam splitter, MO: microscope objective, L: lens, SLM: phase-only spatial light modulator, M: mirror, DM: dichroitic mirror, CMOS: video camera, red: laser light, yellow: white light illumination, green: fluorescence illumination.

The key components of the HOT (red beam path in figure 1) are a 2.5W Nd:YVO_4 cw solid state laser providing a biocompatible [13] wavelength of $\lambda = 1064$nm. The laser light is modulated by an LCOS phase-only spatial light modulator (SLM, 1920x1080 px, max. phase shift $\Delta\varphi > 2\pi$), which is working in reflection geometry with a refresh rate of $\nu =$

60Hz. The modulator is imaged, using a 4f-configuration and a dichroic mirror (DM1), onto the back aperture of the objective (MO2). The objective is a 100times infinity-corrected oil immersion objective and has a high numerical aperture of NA=1.49. The HOT are integrated into the inverted microscope, where a high-speed CMOS camera is positioned to observe the trapping plane. A recording rate of up to 1600 Hz is possible with the available white light illumination, using an area of interest of 320x256px. According to the Nyquist sampling theorem, frequencies up to $f_{Nyq} =$ 800 Hz can be resolved at a recording rate of $f_{sampling}$ = 1600 Hz. The microscope provides fluorescence illumination, and the fluorescence signal can be detected with an additional CCD camera (not shown in the figure) with high quantum yield.

The computation of the holograms is carried out by the "lenses and gratings" algorithm [14], as it is provided in the LabView-based software of the University of Glasgow [15]. A user-friendly interface allows the full control over many traps both simultaneously and separately [11].

3 MEASURING THE ROTATION PROPERTIES OF OPTICAL TRAPPED BACTERIA

Elongated particles, in the size range of the used *B. subtilis* bacteria, will orientate in an optical trap with their major axis always parallel to the beam axis (see figure 2(a)) [16,17]. A rod-shaped bacterium is captured stable in this kind of trapping position [11]. A single bacterium or multiple bacteria trapped in this orientation by means of holographic optical tweezers is the onset of our analysis scheme.

Before we go into the details of the rotation frequency analysis, we have a closer look at the bacteria and their flagella under light exposure in an optical trap. As the flagella's diameter is in the order of a few ten micrometers [12], they are not directly visible with optical microscopy. It is, however, possible to stain the flagella with appropriate fluorescence dyes and thus obtain information of their position and behaviour in an optical trap [7, 11].

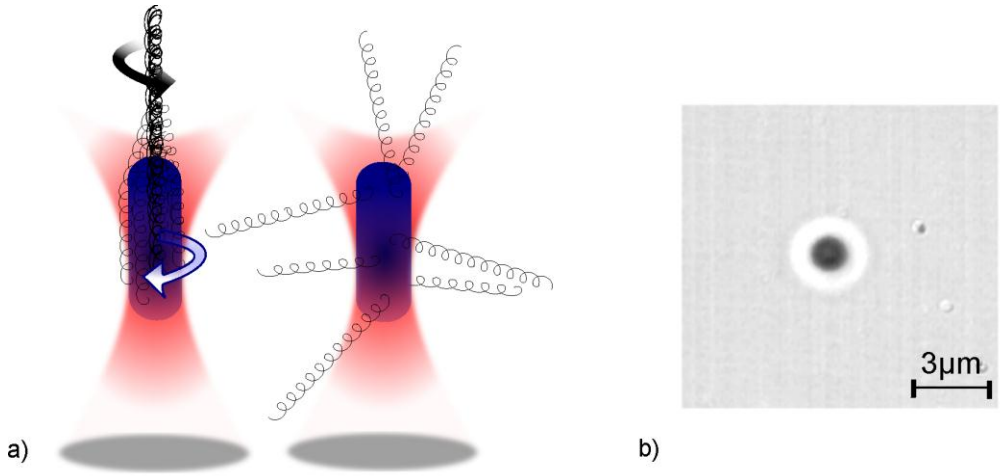

Figure 2. Schematic of an optically trapped bacterium. (a) left: running, right: tumbling bacterium, (b): Top view of trapped bacterium observed through the microscope system.

Figure 3 shows fluorescence images of a bacterial movement in time steps of 0.4 seconds for each subfigure. Initially, the bacterium swims freely from the top left of the figures to the right, reorients itself by means of a tumbling event, and subsequently swims to the left bottom, where it is caught in an optical trap. Only the flagella are marked with the fluorescent dye (green fluorescent CF^{TM} 488A, NHS Ester of Maleimide Alexa), and the bacterial body cannot be seen in the images. In subfigures (a) - (d), the flagella bundle is visible while it is pushing the bacterium forward [6, 8]. In subfigures (g) – (p) the bacterium is optically trapped, and the bundling and unbundling of the flagella can be observed. During this time, the flagella keep leaving and reentering the optical trap. Apparently, the flagella are not significantly influenced by the optical trap. The flagella of the optically trapped bacterium behave similar to those of freely swimming bacteria, indicating that – in agreement with the literature [7] – the bacterial motility is not disturbed by an optical trap.

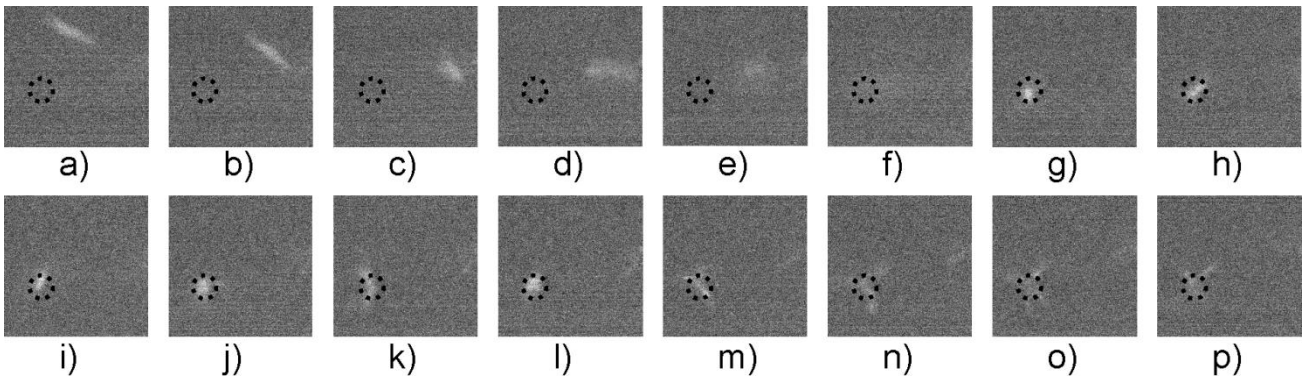

Figure 3. Fluorescence images of a bacterial movement over 6 seconds. Only the flagella are fluorescent. The dashed circles indicate the position of an optical trap. The bacterium swims freely (a-f), and then interacts with the optical trap that confines the bacterial body's position (g-p). In the optical trap, the flagella exhibit "run" and "tumble" states as indicated by the labelled flagella.

The behaviour of a *B. subtilis* cell in an optical trap thus can be understood as indicated in figure 2(a). Although the bacterium is confined, it can switch between its natural run and tumble states. In particular, the body is free to rotate around its long axis during running. The flagella bundle rotates counterclockwise with an angular velocity ω, while the body is counterrotating with a (lower) angular velocity Ω and thus cancelling out the net torque on the bacterium [18].

In general, there are two ways to analyse the rotation frequencies of the bacterial body and the flagella. The first way relies on the fluorescent labelling of the flagella, similar to the situation shown in figure 3. With sufficiently high video frame rates and a higher sensitivity than we can achieve with our camera, it actually is possible to analyse the rotational motion frame-by-frame and thus determine the rotation frequency of the flagella bundle or individual flagella [2, 6, 7]. This direct observation, however, is limited to short observation times or low temporal resolution because the light introduced by the fluorescence illumination is an issue and, furthermore, frame-by-frame analysis is a very time-consuming task.

The second way to determine rotation frequencies from rotating bacteria is the observation of small vibrations [9] of the cell body during the running state. Since the bacterium in general does not have a perfectly symmetric shaped body and flagella distribution, the flagella bundle rotation axis does not match exactly with the body rotation axis [2]. Thus, the rotating bacterium is an asymmetrically rotating system and shows "wobbling" [2], which results in a slight circular motion of the bacterium's centre position. The rotation frequency of the bacterial body of optical trapped bacteria and its flagella and thus its nanomotors can be measured by the temporally-resolved monitoring of the position of the bacterial body. Conventionally, the lateral (x, y; if z is the axis of the optical trap) position is determined indirectly by the deflected laser beam using a semiconductor position sensor (quadrant photodiode) [7, 10]. Plotting the x- and y-position data against time results in sinusoidal curves shifted with respect to each other by $\pi/2$, revealing a rotational movement [10]. The rotation frequencies that can be determined from the movement of the bacterial body are obtained by a complex Fourier transform $F(\omega) = F\{f(t)\}$ of the position data $f(t) = x + iy$. The power spectrum of a rotating bacterium is expected to reveal two different frequencies (Ω, ω) with different signs, corresponding to the counter-rotation of body and flagella. The rotation of the flagella bundle can be accessed because their high frequency rotation results in an additional vibration on top of the low frequency "wobbling" of the cell body. Conceptual reasons, however, usually limit the position detection to the study of only a single bacterium at a time. If polarization as an additional degree of freedom is added, a maximum of two bacteria using two laser traps polarized perpendicular to each other [19, 20] can be realised.

High speed video microscopy methods and appropriate digital post processing on the other hand enable the measurement of the body and the flagella rotation rate of multiple bacteria simultaneously without the use of an additional laser [7]. In the following discussion we present a complementary method that relies on extracting the position data directly from video images similar to figure 2(b). In principle, the video-based concept can be extended to almost arbitrary numbers of bacteria visible in the field of view as long as they can be recognised as separated objects in the video data [22]. Together with the capability of HOT to trap multiple bacteria at defined positions, this concept should result in a highly versatile platform to measure rotation properties of multiple bacteria at the same time and observe possible interactions.

4 DIGITAL IMAGE PROCESSING OF VIDEO DATA

For the video-based rotation analysis, images of optically trapped bacteria are captured with a frame-rate of 1600 Hz. For our model bacterium, *B. subtilis*, we expect body frequencies Ω in the order of a few 10 Hz and rotation frequencies ω of the flagella bundle in the order of a few hundred Hz [21]. Following the Nyquist sampling theorem, we should be able to detect rotation frequencies of up to 800 Hz.

In figure 4(a), one typical video frame is presented, showing four bacteria which are trapped with HOT. In the image, the detected centre positions are marked for each bacterium. The position of the bacteria is determined by a circle detection algorithm, the circular Hough-transformation [22]. The circular Hough-transformation is based on a voting process [22] indicating the most probable centre position of all circles in an image. The votes are transferred to the "accumulation array" (figure 4(b)). Peaks in the accumulation array are points with the highest number of votes and therefore represent the most probable centre points for the searched circle shape. The brightest points thus correspond to the most probable bacteria positions. By appropriate correlation, the position data of each bacterium over the entire video is recorded. Tracking of the bacteria positions works very reliable in all our experiments with some tens of bacteria. It is straightforward to extend the position detection to almost any number of bacteria visible in larger fields of view.

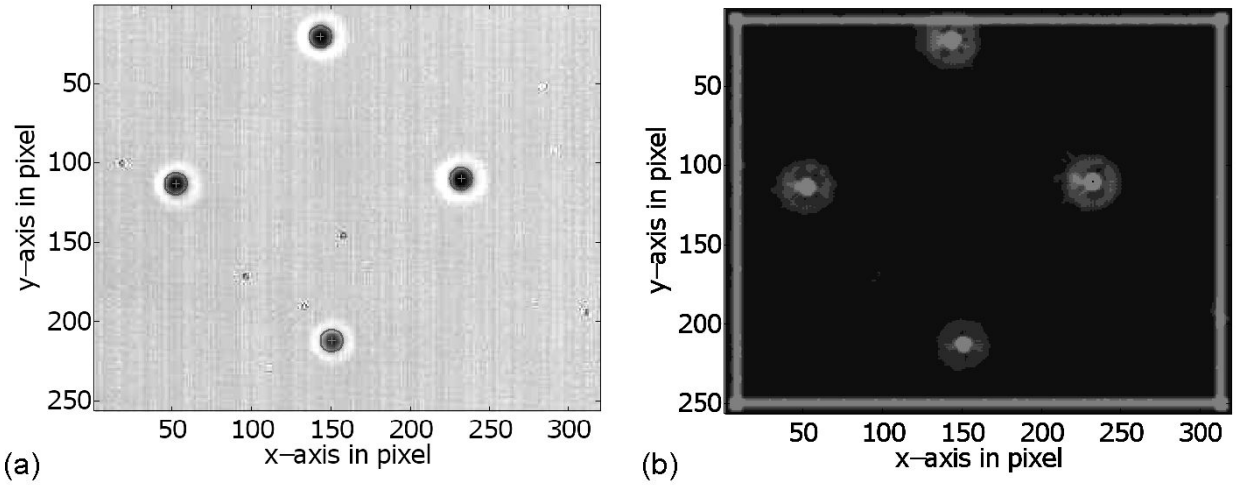

Figure 4: Four optically trapped bacteria tracked by video imaging and subsequent image-processing. (a) Video image with the positions and centres marked for the four visible bacteria. (b) Corresponding accumulation array of the "circular Hough transformation". The brightest points correspond to the most probable bacteria centre positions.

In figure 5(left), a single bacterium of the configuration in figure 4 is depicted. Next to it, the x and y-positions of the bacteria's centre are plotted versus time (figure 5(right)). On both axes, sinusoidal curves can be observed which are shifted by $\pi/2$ with respect to each other. This low frequency signal can be identified as the circular movement due to the body roll frequency Ω. While Ω can be determined by simply counting the full cycles, there are additional modulations on top of the main course which require an analysis in the frequency domain. These higher frequency components are introduced by general noise in the measurement, by the rotational motion of the flagella bundle and by the Brownian motion of the bacteria. We should note that the amplitude of the body movement due to the "wobbling" is only about 2-3 pixels and the amplitude of the higher frequency components is well in the sub-pixel regime. In order to visualise the typical amplitudes we have indicated the complete trajectory of the particle's positions (400 data points) during one measurement (0.25 s) in figure 5(left).

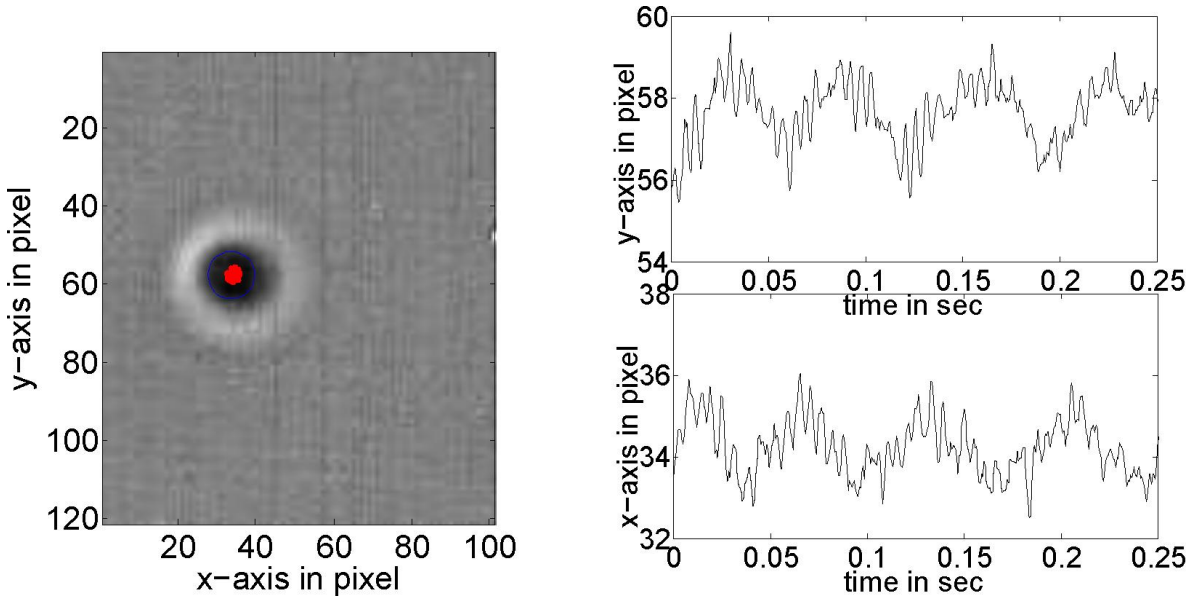

Figure 5: Single bacterium tracked by video analysis. Left: a video frame showing a single bacterium. Red dots represent tracked position in each frame Right: the x-and y-positions of the bacterium's midpoint plotted against time.

5 DETERMINATION OF THE ROTATIONAL FREQUENCIES

The rotation frequencies that can be extracted out of the complex rotation of the bacterial body are obtained by a complex Fourier transform of the position data. In figure 6, the power spectrum $P(\omega) = F(\omega) * \bar{F}(\omega) / T$ of the position data of a tracked bacterium from a short video sequence of T = 0.25 seconds is shown. The data was obtained at a sampling rate of 1572Hz, and each data point shown in the spectrum represents the mean value of 30 data points.

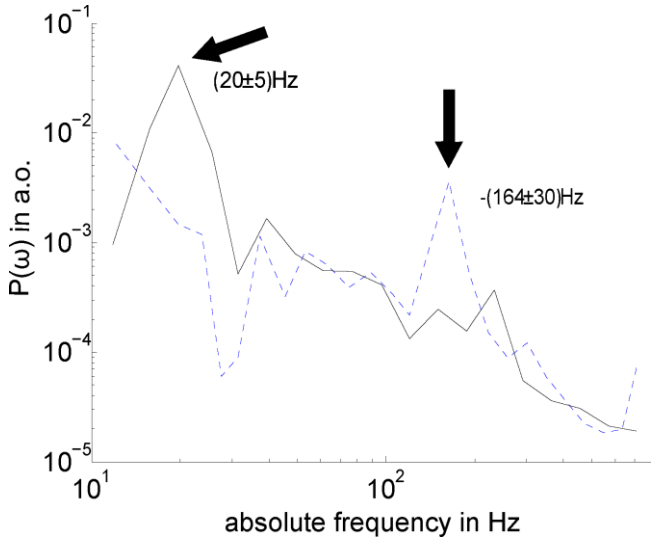

Figure 6. Power spectrum P(ω) of the rotating bacterium, the solid curve corresponds to the positive frequencies, the dashed curve to the negative frequencies.

Since the bacteria's body and flagella rotate in different directions, both positive and negative frequencies need to be considered in the power spectrum. The solid curve corresponds to positive frequencies, the dashed curve to absolute

value of the negative frequencies. In the present example, the positive frequency shows a maximum at (20±5) Hz, the negative frequency at -(164±30) Hz. These rotation frequencies are in the expected range for the body rotation rate Ω and the flagella bundle rotation rate ω, respectively [21]. In order to verify that the identified peaks actually correspond to the searched frequencies, we performed a number of control tests. First, the frequencies were determined for the same bacterium at different times, and for different bacteria. It turned out that the measured flagella bundle frequencies always were in the same orders of magnitude, varying only a couple of tens of Hz in full agreement with the expected behaviour of a living system [2], and in contrast to other noise frequencies which were stationary (see below).

As further verification, the power spectrum of an inactive bacterium (figure 7(a)) is compared with the spectrum of an active bacterium (b). Comparing the power spectra of both states shows that only the active bacterium exhibits very clear peaks at two distinct frequencies. In contrast, the power spectrum of the inactive bacterium is dominated by the pure Brownian motion of a passive bacterium [23].

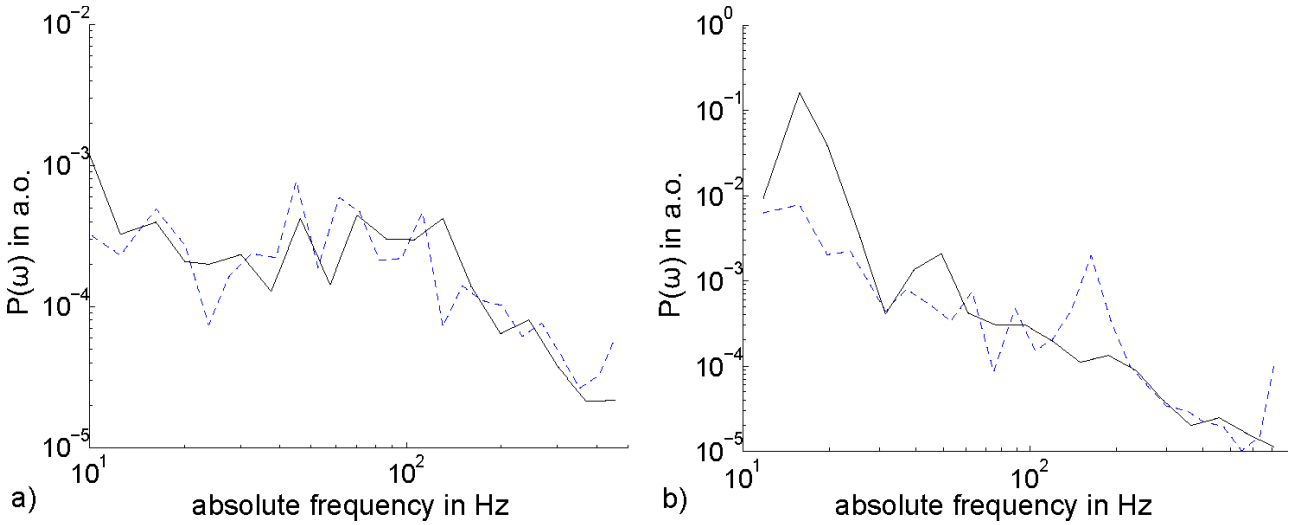

Figure 7. (a) power spectrum of an inactive bacterium,(b) power spectrum of an active bacterium, the black curve corresponds to the positive frequencies, the blue dashed curve to the negative frequencies.

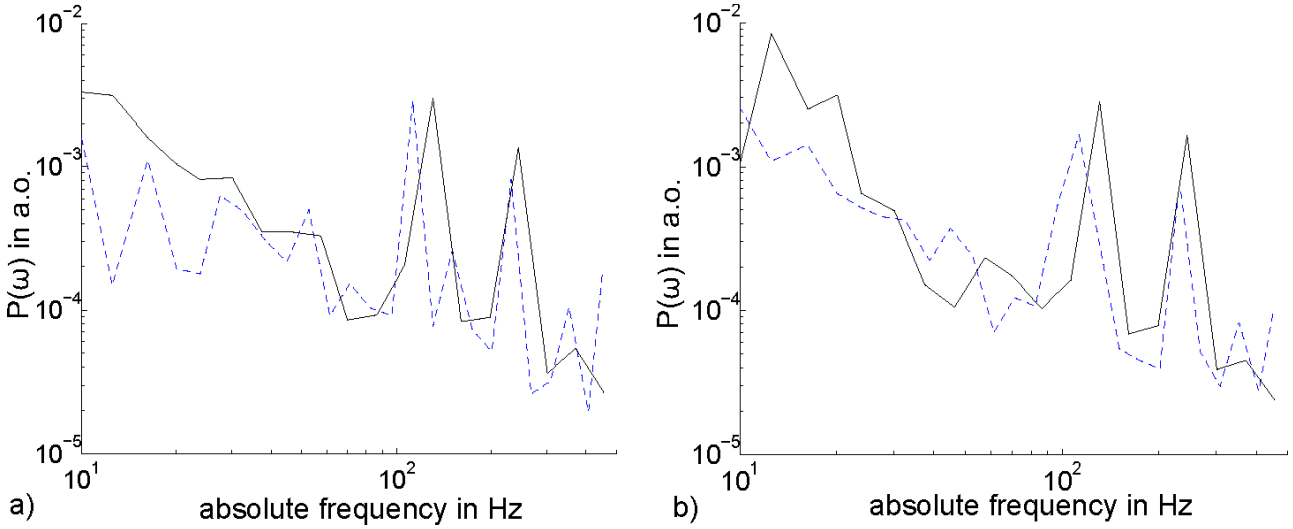

Figure 8: Frequency spectrum of a measured bacterium at two points in time, the black curve corresponds to the positive frequencies, the blue dashed curves the negative frequencies.

Finally, we sometimes observed strong noise peaks at fixed positions in the spectrum (see figure 8 for two examples). This usually happens when observing bacteria which are trapped very close to the zeroth diffraction order of the HOT system. The noise frequencies occur at fixed positions (120 Hz and higher harmonic frequencies), are constant even for longer times, and finally, are symmetric for negative and positive frequencies. These characteristic noise frequencies can be attributed to the digital addressing scheme of the employed SLM, which uses pulse-width modulation and introduces "phase-flicker" [24]. Owing to their characteristics, the noise frequencies introduced by the SLM can be identified easily, and can be distinguished clearly from, for example, rotation rates of flagella bundles which are in a similar frequency range. In order to circumvent this issue we are avoiding trapping in the zeroth order of the holographic optical tweezers.

6 LIMITS OF BACTERIAL ROTATION DETECTION

The method presented here works reproducibly in the sense that for a bacterium which is investigated for a longer time, plausible rotation frequencies within the expected range for the employed bacterial model are measured during the whole observation. Furthermore, several bacteria were investigated successively under similar biological conditions and all determined rotation frequencies of the cell body and the flagella bundle are in a reasonable range as reported by [21]. Clear indications for a successful analysis are the two characteristic peaks in the spectrum which have opposing signs, corresponding to the counterrotating body and flagella bundle, respectively.

However, it turned out the probability to measure the rotation frequencies of a randomly selected bacterium successfully, i.e. with a reasonable signal-to-noise ratio, is relatively low (in the order of a few percent). Similar to our observation, it was reported for conventional detection methods that not every given bacterium yields a sufficient signal-to-noise ratio for the rotational analysis [10]. The low probability therefore seems not to be a conceptional problem of the presented video-based analysis.

Since with our method high-speed video data (and not only position data) of all analysed bacteria exist, however, a detailed video analysis of the origins of this issue becomes possible. Our analysis shows that the successfully measured bacteria (all bacteria where both the body and the flagella frequency can be measured unambiguously) show a characteristic behaviour in the optical trap.

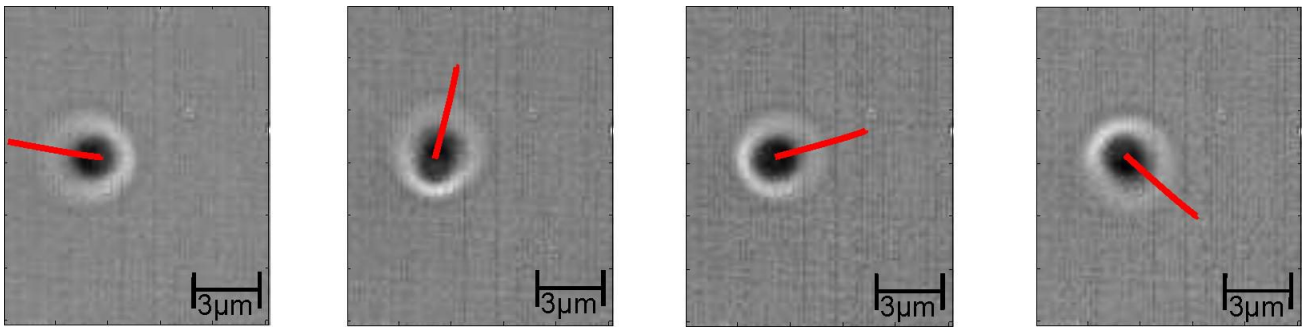

Figure 9. Four snapshots of a "measurable" bacterium in an optical trap. Red lines act as guide to the eye to follow the eccentricity and rotation angle.

Figure 9 shows a typical video sequence of an experiment where the rotation frequencies were measured with a particularly high signal-to-noise ratio. It is clearly seen that the trapped bacterium rotates in a strongly eccentric way, visible even with the naked eye. Apparently, in these cases an especially strong asymmetry of the bacterium results in particularly strong eccentricity of the rotation.

This raises the interesting question of how we could increase the asymmetry of the rotation and thus the "wobbling" on purpose in order to be able to measure the rotation of a randomly selected bacterium with a higher probability. This would be an important step towards the successful measurement of the rotation properties of multiple bacteria simultaneously. Certainly the current setup and the accuracy of the video post processing can be refined to some extend in order to improve the signal-to-noise ratio but as the problem seems to be inherent [10] and not specific to our scheme, it might be

necessary to consider further improvements. Possible solutions would be to introduce asymmetric optical trapping potentials wells (in contrast to the highly symmetric optical trap commonly employed in HOT), or to increase the bacterial body's natural asymmetry artificially or by carefully selecting a suited strain of the bacterium under investigation.

7 SUMMARY

In this contribution, we presented an experimental platform for the investigation of bacterial rotational properties of a multitude of bacteria in parallel. The basic idea is to extract the rotation frequencies of bacterial body and flagella bundle from position data of the body. In contrast to previous studies we have used HOT and investigated the use of video-based data analysis which is an important step towards the detection and investigation of multiple bacteria within the field of view. The possibility of monitoring the behaviour of multiple bacteria simultaneously provides the potential to study their hydrodynamic interactions, including possible cooperative effects and the resulting spatio-temporal dynamics directly from their rotational behaviour. While we did not yet achieve the final goal, we have shown that the video-based scheme is a promising approach and only the low probability that a randomly selected bacterium can be measured successfully prevents the simultaneous measurement of multiple bacteria at the same time. This low probability is not unique to the video-based approach. On the contrary, using the video data we have shown that it results from the relatively low natural asymmetry of the used model organism. Further studies thus can help to identify conditions where the reliability of rotation measurement schemes in general can be improved.

ACKNOWLEDGEMENT

The authors would like to thank Jan Ribbe and Berenike Maier, University of Cologne, for kindly supplying *B. subtilis* samples and Florian Hörner, University of Muenster, for helpful discussions. The work was partly supported by the Deutsche Forschungsgemeinschaft within the Collaborative Research Centre / Transregio 61, project C1 "Cooperative interactions of molecular rotational motor complexes"..

REFERENCES

[1] Berry, R.M., "Bacterial flagella: Flagellar motor" Encyclopedia of life sciences (2001)

[2] Darnton, N.C., Turner, L., Rojevsky, S. & Berg, H. C., "On Torque and Tumbling in swimming Escherichia coli" Journal of Bacteriology, 189, 1756-1764 (2007)

[3] Berg, H.C., "The rotary motor of bacterial flagella" Annual Review of Biochemistry, 72,19–54 (2003)

[4] Chen, X. & Berg, H. C. „Torque-speed relationship of the flagellar rotary motor of escherichia coli" Biophysical Journal, 78, 1036 (2000)

[5] Rao, C.V., Kirby, J.R. & Arkin, A.P., "Design and Diversity in Bacterial Chemotaxis: A Comparative Study in Escherichia coli and Bacillus subtilis" PLOS Biology, 2(2), 239-252 (2004)

[6] Turner, L., Ryu, W.S. & Berg, H.C., „Real-Time Imaging of Fluorescent Flagellar Filaments" Journal of Bacteriology, 182(10), 2793-2801 (2000)

[7] Min, T.L., Mears, P.J., Chubiz, L.M., Rao, C.V., Golding, I. & Chemla, Y.R.. "High resolution, long-term characterization of bacterial motility using optical tweezers" Nat Methods, 6(11),831–835 (2009)

[8] Altindal, T., Chattopadhyay, S. & Wu, X. L.. "Bacterial chemotaxis in an optical trap" PLos One, 6(4), 1-12 (2011)

[9] Lowe, G., Meister, M. & Berg, H. C. “Rapid rotation of flagellar bundles in swimming acteria” *Nature*, 325, 637 – 640 (1987)

[10] Rowe, A. D., Leake, M. C., Morgan, H. & Berry, R. M. “Rapid rotation of micron and submicron dielectric particles measured using optical tweezers” J. Mod. Opt., 50, 1539-1554 (2003)

[11] Hörner, F., Woerdemann, M., Müller, S., Maier, B. & Denz, C. “Full 3D translational and rotational optical control of multiple rod-shaped bacteria” J. Biophoton., 3, 468-475, (2010)

[12] Cisneros, L., Cortez, R., Dombrowski, C., Goldstein, R. & Kessler, J. “Fluid dynamics of self-propelled microorganisms, from individuals to concentrated populations” *Exp. Fluids*, 43, 737-753 (2007)

[13] Ashkin, A., Dziedzic, J. M. & Yamane T. “Optical trapping and manipulation of single cells using infrared laser beams” Nature, 330, 769-771 (1987)

[14] Liesener, J., Reicherter, M., Haist, T. & Tiziani, H. “Multi-functional optical tweezers using computer-generated holograms” *Opt. Commun.,* 185, 77-82 (2000)

[15] Leach, J., Wulff, K., Sinclair, G., Jordan, P., Courtial, J., Thomson, L., Gibson, G., Karunwi, K., Cooper, J., Laczik, Z. J. & Padgett, M. "Interactive approach to optical tweezers control," Appl. Opt. 45, 897-903 (2006)

[16] Benito, D.C., Simpson, S.H. & Hanna, S.. “Fdtd simulations of forces on particles during holographic assembly” Optics Express, 16(5), 2942-2957 (2008)

[17] Simpson, S.H. & Hanna, S.. “Computational study of the optical trapping of ellipsoidal particles” Physics Review A, 84(5), 053808(11) (2011)

[18] Kim, M., Bird, J.C., Van Parys, A.J., Breuer, K.S. & Powers, T.R., “A macroscopic scale model of bacterial flagella bundling” PNAS, 100, 15485 (2003)

[19] Visscher, K., Gross, S. P. & Block, S. M. “Construction of multiple-beam optical traps with nanometer-resolution position sensing” IEE Journal Of Selected Topics In Quantum Electronics, 2, 1066 –1076 (1996)

[20] Moffitt, J. R., Chemla, Y. R., Izhaky, D. & Bustamante, C.. “Differential detection of dual traps improves the spatial resolution of optical tweezers” PNAS, 103, 9006-9011 (2006)

[21] Cisneros, L. H., Kessler, J. O., Ortiz, R., Cortez, R. & Bees, M. A. “Unexpected Bipolar Flagellar Arrangements and Long-Range Flows Driven by Bacteria near Solid Boundaries” Phys. Rev. Lett., 101, 168102 (2008)

[22] Illingworth, J. & Kittler, J. “A Survey of the Hough Transform“ Computer vision, graphics, and image processing 44, 87–116 (1988)

[23] Berg-Sørensen, K. & Flyvbjerg, H. “Power spectrum analysis for optical tweezers” Rev. Sci. Instrum., 75, 594-612 (2004)

[24] Hermerschmidt, A., Osten, S., Krüger, S. & Blümel, T., “Wave front generation using a phase-only modulating liquid-crystalbased micro-display with HDTV resolution” Proc. SPIE 6584, 65840E (2007)